Relaxed-Bound K-Best Sphere Detection for Differential Unitary Space-Time Modulation

Yipeng Du[1], Shuangshuang Han[2], Jian Liu[1], and Yinghua Zhang[1]
[1]School of Computer & Communication Engineering, University of Science and Technology Beijing, Beijing, China
[2]The State Key Laboratory of Management and Control for Complex Systems,
Institute of Automation, Chinese Academy of Sciences, Beijing, China.
Email: 41456007@xs.ustb.edu.cn, shuangshuang.han@ia.ac.cn, liujian@ustb.edu.cn, zhangyh@sugon.com

***Abstract*—Large scale multiple input multiple output (MIMO), commonly referred to as massive MIMO, is one of the most important physical layer disruptions in network evolution that would lead to significant increase in spectral and energy efficiency envisioned for 5G networks. However, the computational complexity of massive MIMO system becomes the key problem for its practical implementation. As known, Differential Unitary Space-Time Modulation (DUSTM) has been proposed as an efficient modulation choice for such MIMO transmissions where channel state information (CSI) is not required at the receiver. However, traditional DUSTM implementation relies mainly on Maximum Likelihood Detection (MLD) achieving optimal performance, which is not easily compatible with massive MIMO systems due to its exponentially increasing complexity with increasing number of transmitting and receiving antennas. Therefore, in this paper, in order to overcome the aforementioned disadvantages, we propose a new detection algorithm named Relaxed-Bound K-Best Sphere Detection (RBKSD). Compared to the traditional K-Best Sphere Detection (KSD) algorithm, the main idea of our algorithm is to relax the bound K of the conventional KSD to be $K + \Gamma$, thereby achieving quasi-optimal performance with significantly reduced computational complexity. Simulation results confirm that the proposed RBKSD algorithm shows superior performance and reduced complexity compared to other notable schemes such as MLD, traditional sphere detection algorithm and the KSD.**

I. Introduction

In recent years, advances in the physical layer with respect to antenna technologies are yielding very high data rates with low error probabilities for multiple-antenna communication links, especially when the wireless channel response is known at the receiver. However, the continuous-assumption that channel state information is readily available is often idealistic, since perfect channel estimation is either costly or even impossible in complex and fast-changing channel conditions. This is especially true for multiple input multiple output (MIMO) systems and even more so for massive MIMO transmissions. The traditional modulation schemes may no longer be reliable in such conditions. This motivates researchers to find new types of modulation schemes without knowledge of channel estimates. In this context, differential unitary space-time modulation (DUSTM) emerges as an appropriate candidate scheme [1-5].

The basic principle of DUSTM is to encode the transmitted information into phase differences between two consecutively received symbols, and at the receiving end, we can decode the information by comparing the phase between the currently accepted symbol and the previous accepted symbol [3-4]. In this way, the signals can be used to achieve lower probability of error without knowledge of channel estimates. What's more, DUSTM can also be applied to different channels [6-8].

As one important topic, detection of DUSTM is usually based on two consecutively received symbols, which is referred to as conventional differential detection (CDD)[9-14]. As the optimal detection method, maximum likelihood detection (MLD) is widely used to decode the differential unitary space-time signals [15-19]. By the aid of MLD, performance of the decoder can be made better than CDD. However, the complexity of the MLD algorithm using exhaustive search increases exponentially with the number of antennas. This will result in a high degree of complexity, making the scheme difficult to implement. The emergence of the sphere detection (SD) algorithm resolves these challenges with moderate complexity [20-22].

The main advantage of SD algorithm is that it only needs to search in a predetermined finite spherical region instead of searching all the grid points in the whole box [23-25]. However, use of the depth-first tree search in the SD algorithm limits the decoding efficiency in non-constant throughput [26-28]. Furthermore, the complexity of the SD algorithm increases rapidly when SNR changes from high to low.

Therefore, another SD detection algorithm called K-best sphere detection (KSD) algorithm is proposed, which is based on tree search to obtain the log likelihood ratio (LLR) of two Euclidean distances. Unlike the conventional SD, the KSD performs a breadth-first search strategy and retains only K best nodes at each layer instead of a depth-first tree traversal. The KSD algorithm selects only the specified surviving paths in all paths as the next path to be computed.

For DUSTM, KSD has received significant attention recently due to its fixed throughput, fixed detection, computational complexity and parallel implementation. Despite these advantages, the KSD typically requires very large values of K to guarantee an optimal performance, which results in a higher computational complexity than that of the conventional SD.

The performance loss of the KSD may be due to the

likelihood of inadvertently discarding the ML solution. In this paper, we propose a relaxed-bound K-best sphere detection (RBKSD), which replaces the strict value K in the conventional KSD with a hyper-sphere radius determined by the cost of the K-th best node and a threshold. The proposed RBKSD requires a smaller K value while still achieving a better and near optimal performance compared to the conventional KSD with a larger K. The RBKSD achieves a near-optimal performance with a much lower computational complexity than that of the conventional KSD.

Unlike the conventional KSD which keeps K nodes for each layer, the RBKSD searches the fixed K nodes and all nodes with a partial cost equal to or less than the K-th node cost plus a small value Γ. The parameter Γ controls the extra number of nodes visited by the RBKSD. The RBKSD expands the fixed K nodes at each layer to a slightly bigger list, which includes all the nodes with a partial cost of $newdist$ equal to or less than the K-th node cost $newdist_K$ plus a small value Γ. This Γ could be derived by off-line computation. Furthermore, the RBKSD increases the possibility of the candidate list including the optimal ML point and reduces the complexity with close performance to the conventional KSD detection.

The rest of the paper is organized as follows. Section II outlines the system model. In section III, we analyze several conventional detection algorithms for differential unitary space-time modulation. We introduce our relaxed-bound K-Best SD algorithm in section IV while the simulation results and discussions are presented in section V. Finally, Section VI concludes this paper.

II. System Model

We consider a DUSTM system using N_{T} transmitter antennas and N_{R} receiver antennas, and use R (bits/channel use) to represent the data rate in bit per channel use. At the transmitter $N_T R$ bits of signals are organized into a $(N_{\mathrm{T}} \times N_{\mathrm{T}})$ -dimensional unitary matrix $\boldsymbol{G}[\eta]$, which has the form

$$\boldsymbol{G}_l = \boldsymbol{G}_1{}^l, \quad \boldsymbol{G}_1 = \mathrm{diag}\left\{ e^{\frac{j2\pi\mu_1}{L}}, ..., e^{\frac{j2\pi\mu_{N_T}}{L}} \right\}, \quad 0 \le l \le L-1, L = 2^{N_T R}. \tag{1}$$

The generator $\mathbf{u} = \{1, u_2, u_3, ..., u_{N_T}\}$ could be derived to maximize the diversity product [4]. The data symbols $\boldsymbol{G}_l[\eta]$ are then differentially encoded into transmit symbols

$$\boldsymbol{S}[\eta] = \boldsymbol{G}[\eta]\boldsymbol{S}[\eta-1], \quad \boldsymbol{S}[0] = \boldsymbol{I}_{N_{\mathrm{T}}}. \tag{2}$$

Subsequently, a $(N_{\mathrm{R}} \times N_{\mathrm{T}})$ channel matrix $H[\eta]$ is defined where $h_{i,j}[\eta]$ denotes the complex fading gain between transmit antenna j and the receive antenna i. The fading channels are assumed to be spatially uncorrelated with identical temporal correlation according to Clarke's fading models[12].

According to the model, the received signals can be expressed by $Y[\eta] = H[\eta]S[\eta] + N[\eta]$. The $n_{i,j}[\eta]$ of $N[\eta]$ denotes the zero-mean complex additive spatially and temporally white Gaussian noise(AWGN) with variance $\sigma^2 = N_0/T$ effective at the receive antenna at time η. While N_0 is the two-side noise-power spectral density in the equivalent complex baseband (ECB) and the $NN_R \times N_T$ matrix $\bar{Y}[\eta]$ of N received matrix symbols can be expressed as

$$\bar{Y}[\eta] = \bar{H}[\eta]\bar{S}_D[\eta] + \bar{N}[\eta], \tag{3}$$

where the $NN_T \times NN_T$ matrix block -diagonal matrix is given by $\bar{S}_D[\eta] \triangleq \mathrm{diag}\{S^T[\eta-N+1], ..., S^T[\eta]\}$, the $NN_R \times N_T$ matrices given by $\bar{H}[\eta] \triangleq \mathrm{diag}\{H^T[\eta-N+1], ..., H^T[\eta]\}$ and $\bar{N}[\eta] \triangleq \mathrm{diag}\left\{N^T[\eta-N+1], ..., N^T[\eta]\right\}$, respectively.

III. Detection Algorithms

In this section, we first provide a suitable representation of the ML decision rule in Section III-A. Subsequently, the SD algorithm and the conventional KSD are presented.

A. Maximum-likelihood Detection

Single-symbol differential ML detection processes two consecutively received matrix symbols to find ML estimates for the data symbols $\bar{V}[\eta] \triangleq [G^T[\eta-1], G^T[\eta]]^T$, which is correspond to the transmit symbols $\bar{S}[\eta] \triangleq [S^T[\eta-1], S^T[\eta]]^T$. For brevity, we will henceforth omit the reference $[\eta]$ to time in some of the following mathematical formulas.

In [4], the ML demodulator for a constellation of unitary space-time signals is defined as a matrix noncoherent correlation receiver, given as

$$V_{ml} = \arg \max_{V_l = V_0, ..., V_{L-1}} \left|\left| V_l Y^H \right|\right|, \tag{4}$$

where $2N_T \times N_T$ matrices V_l obey $V_0^H V_0 = \cdots = V_{L-1}^H V_{L-1} = I_{N_T}$ According to $Y[\eta] = H[\eta]S[\eta] + N[\eta]$, the maximum-likelihood demodulator is:

$$\begin{aligned} (\hat{z}_\eta)_{ml} &= \arg \max_{l=0,...,L-1} \left|\left| V_l Y^H \right|\right| \\ &= \arg \max_{l=0,...,L-1} \left|\left| Y[\eta-1] + Y[\eta] G_l^H \right|\right|, \end{aligned} \tag{5}$$

where $Y[\eta]$ is an $N_R \times N_T$ matrix. Demodulation requires looking at two successive matrices to form a matrix with $T = 2N_T$ rows as [4]

$$Y = \begin{bmatrix} Y[\eta-1] \\ Y[\eta] \end{bmatrix}. \tag{6}$$

For the case of multiple-symbol differential ML detection, according to (3) and the fact that $\bar{S}_D[\eta]$ denotes an unitary matrix, we an obtain multiple-symbol differential ML detection rule

$$\hat{\bar{G}} = \arg \min_{\bar{G}} \left\{ \sum_{n=1}^{N-1} \left|\left| \bar{G}_n \tilde{Y}_{n,n} + X_n \right|\right|^2 \right\} \tag{7}$$

with

$$X_n = S_{n+1} \sum_{j=n+1}^{N} S_j^H \tilde{Y}_{n,j}, \tag{8}$$

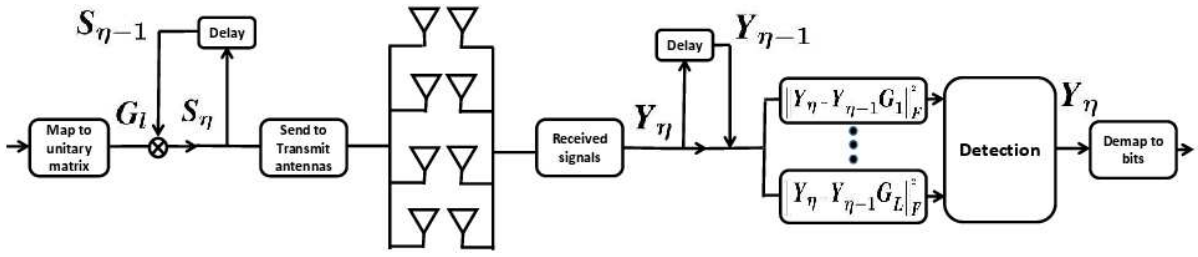

Fig. 1 DUSTM system model.

where $\tilde{Y}_{n,j} \triangleq \frac{p_{j-i}^{(N-i)}}{\sigma_e^{N-i}} Y_j$. $p_j^{(i)}$ denotes the j-th coefficient of the i-th order linear backward minimum mean-squared error (MMSE) predictor for the discrete time random process $h_{\mu,\nu}[\eta N_T] + n_\nu[\eta N_T]$ and σ_e^i denotes the corresponding error variance [12].

We obtain an estimate $\hat{\bar{G}}$ for the vector $\bar{G}$. The brute-force approach can be used to evaluate (7) for all $2^{(N-1)N_T R}\bar{G}$ corresponding to all possible $\bar{G}$. However, this approach wou-ld quickly become computationally infeasible because the complexity of the straightforward approach is exponentially increased in N, the number of transmit antennas N_T and the rate R.

B. Sphere Detection

As earlier mentioned, ML algorithm has an inherent complexity that is exponential in N, N_T, and R [27-28]. We can use SD algorithm to decode from a lattice viewpoint. It can be observed that the ML for diagonal constellations is given by

$$(\hat{z})_{ml}[\eta] = \arg \max_{l=0,\ldots,L-1} \sum_{m=1}^{N_T} \sum_{n=1}^{N_R} Re \times \left[e^{\frac{j2\pi\mu_m l}{L}} y_{n,m}^*[\eta] y_{n,m}[\eta-1] \right]. \tag{9}$$

It is obvious that $e^{\frac{j2\pi\mu_m l}{L}}$ does not depend on index n, thus

$$(\hat{z})_{ml}[\eta] = \arg \max_{l=0,\ldots,L-1} \sum_{m=1}^{N_T} Re \times \left[\left(\sum_{n=1}^{N_R} y_{n,m}[\eta] y_{n,m}^*[\eta-1] \right) e^{-\frac{j2\pi\mu_m l}{L}} \right]. \tag{10}$$

Furthermore, It is given as

$$\Psi_m = \sqrt{\left| \sum_{n=1}^{N_R} y_{n,m}[\eta] y_{n,m}^*[\eta-1] \right|}, \quad \vartheta_m = \frac{L}{2\pi} \arg \left(\sum_{n=1}^{N_R} y_{n,m}[\eta] y_{n,m}^*[\eta-1] \right), \tag{11}$$

where $\vartheta_m \epsilon [-L/2, L/2)$ and $y_{n,m}[\eta]$ is the element of received matrix $Y[\eta]$. Then the simplified expression is derived as

$$(\hat{z})_{ml}[\eta] = \arg \max_{l=0,\ldots,L-1} \sum_{m=1}^{N_T} \Psi_m^2 \cos \left[\frac{(u_m l - \vartheta_m) 2\pi}{L} \right]. \tag{12}$$

Based on some mathematical processes as presented in (12), the best solution can be rewritten as

$$(\hat{z})_{ml}[\eta] = \arg \min_{l=0,\ldots,L-1} \sum_{m=1}^{N_T} [(\Psi_m u_m l - \Psi_m \Phi_m) \mathrm{mod}^* \Psi_m L]^2, \tag{13}$$

If a basis is defined

$$\mathbf{C} = [\mathbf{c}_1, \mathbf{c}_2, \cdots, \mathbf{c}_{N_T}] = \begin{bmatrix} \Psi_1 & 0 & \cdots & 0 \\ \Psi_2 u_2 & \Psi_2 L & \cdots & 0 \\ \vdots & \vdots & \ddots & \vdots \\ \Psi_{N_T} u_{N_T} & 0 & \cdots & \Psi_{N_T} L \end{bmatrix}$$

The point set $\left\{ \mathbf{Cx} : \mathbf{x} \epsilon \mathbf{Z}^{N_T} \right\}$ will form an infinite lattice in $\mathbf{R}^{N_T}$. For easier reading, we define $\mathbf{t}$ as a target with components $\Psi_m \vartheta_m$. So ML decision can minimize the value of $||\mathbf{Cx} - \mathbf{t}||^2$. However, such decoding in an infinite lattice has the convenient feature that is suitable for formulating the SD algorithm, let us define

$$d_k^2 = \sum_{i=k}^{N_T} ||C(k,:)x - t_i||^2. \tag{14}$$

Where $C(k,:)$ denotes the i-th row submatrix of C.

Starting at $k = N_T$, the SD algorithm selects candidates $x_k \epsilon \mathbf{Z}$ and continues to decrease k as long as the current metric d_n does not exceed a given metric ρ_r, such that

$$d_k \leq \rho_r. \tag{15}$$

But if the SD algorithm reaches $k = 1$, we can reduce the size of the search space by updating $\rho_r = d_1$. If d_k exceeds ρ_r for any values of k, k is increased and a new candidate for k is examined. Furthermore, if there are no further candidates inside the current sphere and it means that the ML solution $\hat{x} = x_1 \mathrm{mod} L$ has been found.

C. Conventional K-best Sphere Detection

The conventional SD algorithm uses the depth-first search strategy. Though its performance may be quite optimal, its variable complexity still makes it impossible to apply in practice. That is why the conventional KSD was proposed.

Conventional KSD is not optimal compared to traditional algorithm because it has further reduced the search space and performance is also degraded. Nevertheless, its ability to maintain simpler and non-varying complexity makes its implementation feasible in practical applications. First of all, it is defined as

$$\delta_k^2 \triangleq ||C(k,:)x - t_k||^2 . \quad (16)$$

To formulate the KSD algorithm, the radius is defined as

$$d_k^2 \triangleq \sum_{i=k}^{N_T} ||C(k,:)x - t_k||^2 = d_{k+1}^2 + \delta_k^2. \quad (17)$$

First, it is assumed that the k-th layer of the search tree retains the K-best path corresponding to K vectors: δ_{i_1},...,δ_{i_K}. Then the (k+1)-th layer needs to expand the K nodes, and KSD requires calculation of each child node. Furthermore, for the remaining point of next layer, in an ascending order, K nodes are with the smallest d are maintained while others are deleted. This process is repeated until k = 1, where the last layer of the path with the smallest d is the final path.

IV. Relaxed-bound K-best Sphere Detection

The proposed Relaxed-bound K-best Sphere Detection scheme provides improvements from the conventional KSD scheme in terms of reduced computational complexity as described in the following section.

A. Relaxed-bound K-best Algorithm

Algorithm 1: The RBKSD Algorithm
Input: Γ, C, t, d, K
Output: $\hat{x}$

1. Input Γ, C, t, d, K and initial the sphere radius d is large enough to guarantee that the sphere contains the solution. The partial cost $bestdist$ = 0, level $k = N_T$;
2. **for** i = 1: 1: length ($bestdist$), where i is the number of elements, calculate: $newdist = bestdist_i + \delta_k^2$; $\delta_k^2 = ||C(k,:)x - t_k||^2$; **end**
3. Sort all the calculations of $newdist$ in an ascending order;
4. **if** The number of all sorted $newdist$ is less than K; **then** Keep all the sorted $newdist$ which satisfy $newdist \leq d^2$ to obtain x; **else** Keep the candidates whose cost satisfy $newdist \leq newdist_K$+Γ; **end**
5. Replace the $bestdist$ to be the adjusted *newdist*;
6. **if** $level \neq 1$ **then** Go to step 2 with $k = k - 1$; **else** Return $x_1 \bmod L$ as the estimated $\hat{x}$ **end**

Since the performance loss of the KSD may be due to the likelihood of inadvertently discarding the ML solution, the proposed RBKSD replaces the strict value K in the conventional KSD with a hyper-sphere radius determined by the cost of the K-th best node and a threshold Γ. As a result, the proposed RBKSD achieves a near ML performance with a much lower computational complexity than that of the conventional KSD. As mentioned in Section III, the conventional KSD keeps K nodes for each layer. However, the proposed RBKSD searches the fixed K nodes and all the nodes with a partial cost equal to or less than the K-th node cost plus a small value Γ. Thus, the probability of finding the ML solution is increased compared to the probability of doing so with the conventional KSD.

The detailed process for the proposed RBKSD algorithm is illustrated as follows. $bestdist$ and k indicate the partial cost and the level, respectively. What's more, the radius d is set to be large enough to guarantee that the sphere contains the solution. For each layer, the proposed RBKSD calculates the cost of each point like KSD,

$$\delta_k^2 = ||C(k,:)x - t_k||^2 . \quad (18)$$

Then we can obtain the $newdist$

$$newdist = bestdist_i + \delta_k^2. \quad (19)$$

What's more, we sort all the calculations of $newdist$ in an ascending order. The proposed RBKSD is described in Algorithm 1.

From Algorithm 1, we can obviously see the difference between KSD and the proposed RBKSD. It is obvious that we keep the additional nodes whose costs are close to the cost of the K-th node $newdist_K$ instead of choosing exactly K nodes in KSD. Let us take an example: after sorting the nodes at the k-th layer, if the cost difference between the K-th node and the (K + p)-th node (p = 1,2,...) is less than Γ then all K + p nodes are retained.

B. Complexity Analysis

According to Algorithm 1, it is significant to choose a suitable Γ for this algorithm. If Γ is too large, then more nodes are visited and the computation complexity increases, where as if Γ is too small, the performance improvement is limited compared to of the KSD. In order to achieve a flexible performance and computational complexity trade off, Γ could be predefined and changeable for different system requirement. The choice is motivated by the need to prune less aggressively in the early stage. However, the theoretical complexity analysis is difficult for the proposed RBKSD, because it is infeasible to count the number of nodes within $newdist \leq newdist_K$ + Γ. Therefore, we begin with analysis of the conventional SD algorithm in multi-antenna DUSTM systems.

Since the operation for each possible V is almost the same, the computational complexity denoted by the number of visited points can be defined as [20]

$$\hat{S} = \arg\min_{G} \sum_{i=1}^{N_R} \sum_{j=1}^{N_T} |Y_\eta(i,j) - Y_{\eta-1}(i,m)G(m,j)|^2 , \quad (20)$$

$$\Phi_{ml} = N_T N_R 2^{N_T R}. \quad (21)$$

We define a variance ν for SD

$$\nu(i,j) \triangleq Y_\eta(i,j) - Y_{\eta-1}(i,m)G(m,j) \quad (22)$$

and

$$Y_\eta(i,j) = Y_{\eta-1}(i,m)G(m,j) + n'. \quad (23)$$

Then we have

$$\nu(i,j) \triangleq n' + Y_{\eta-1}(i,m')G(m',j) - Y_{\eta-1}(i,m)G(m,j)\ . \tag{24}$$

We define

$$u(i,j) = Y_{\eta-1}(i,m')G(m',j) - Y_{\eta-1}(i,m)G(m,j). \tag{25}$$

Therefore the probability density function of $\nu(i,j)$ is

$$f(\nu(i,j)|X, Y_{\eta-1}, N_0) \triangleq \frac{1}{\pi N_0} e^{-\frac{|\nu(i,j)-u(i,j)|}{N_0}}. \tag{26}$$

Furthermore, SD algorithm implements the accumulation of distances until the k-th level

$$y(k) = \sum_{\forall(i,j)} |\nu(i,j)|^2. \tag{27}$$

Accordingly, the probability of having a unitary at the k-th level inside the sphere with radius d is

$$P(d,k) = P(y(k) \le d^2 | X_\eta, Y_{\eta-1}, N_0). \tag{28}$$

For the need of analysis we define

$$\Upsilon(k) = \sum_{\forall(i,j)} \frac{|\nu(i,j)|^2}{N_0}. \tag{29}$$

So $P(d,k)$ can be rewritten as

$$P(d,k) = P(\Upsilon(k) \le \frac{d^2}{N_0} | X_\eta, Y_{\eta-1}, N_0). \tag{30}$$

$\Upsilon(k)$ obeys the non-central chi-squared distribution, which has a non-central parameter

$$\Lambda(k) = \sum_{\forall(i,j)} \frac{|u(i,j)|^2}{N_0}. \tag{31}$$

The probability of having a matrix G at the k-th level inside the sphere with radius d can be rewritten by utilizing the generalized Marcum's Q function [13]

$$P_{SD}(k) = 1 - Q_k(\sqrt{\Lambda(k)}, \frac{d}{\sqrt{N_0}}). \tag{32}$$

If $P(N_T)$ is large than the threshold value ρ_r, d is updated by

$$d^2 = \sum_{\forall(i,j)} |n' + u(i,j)|^2\ . \tag{33}$$

Therefore the total computational complexity for DUSTM-SD is

$$\Phi_{SD} = \sum_{G} \sum_{k=1}^{N_T} P_{SD}(k). \tag{34}$$

However, for the KSD algorithm, it keeps just K nodes for each layer. Therefore the total computational complexity for DUSTM-KSD is

$$\Phi_{KSD} = KN_T. \tag{35}$$

While for the proposed RBKSD algorithm, the points selected at each layer are not necessarily the same due to the existence of threshold Γ, so we define a a variance Ω In this situation

$$\Omega = \sum_{G} \sum_{k=1}^{N_T} P(newdist \le newdist_K + \Gamma | X_t, Y_{t-1}, N_0). \tag{36}$$

So

$$\Phi_{RBKSD} = \Phi_{KSD} + \Omega. \tag{37}$$

It is difficult to analyze its computational complexity because of its threshold Γ but we can carry out the actual verification according to simulation results. So we define a variable Θ to measure computational complexity of the proposed RBKSD

$$\Theta(\%) = \frac{\Phi_{SD} - \Phi_{RBKSD}}{\Phi_{SD}} \times 100\%. \tag{38}$$

Θ is measured by the reduced complexity of the proposed RBKSD compared to SD to obtain the same performance.

V. Simulation Results and Discussions

In this section we firstly compare the performance and computational complexity of four detection algorithms (MLD, SD, KS, the proposed RBKSD).

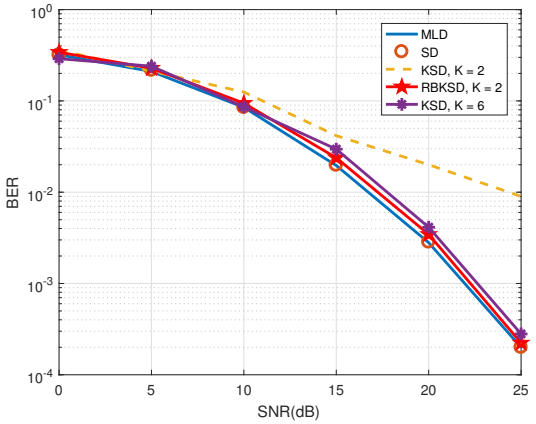

Fig. 2 BER performance comparison among MLD, SD, KSD, the proposed RBKSD for DUSTM.

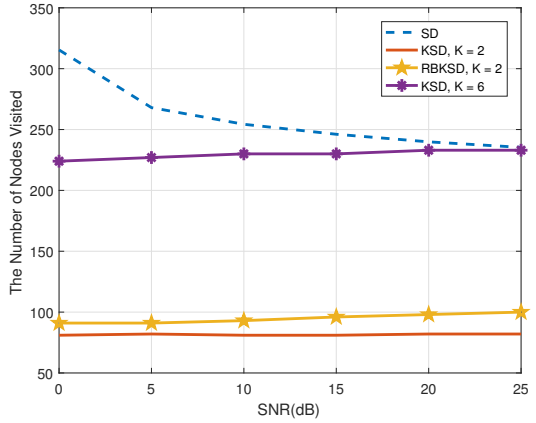

Fig. 3 Computational complexity comparison of SD, KSD, the proposed RBKSD.

Fig. 2 and Fig. 3 show the comparison of the BER performance and computational complexity of four detection algorithms: MLD, SD, KSD, the proposed RBKSD. A DUSTM system in the case of N_R = 4 is simulated over the flat Rayleigh fading channel (σ^2 = 1). It is noted that the BER performance of the proposed RBKSD with index K = 2, Γ = 0.28 is quite close to the MLD performance, while the KSD with same index K = 2 achieves a poorer performance. As for computational complexity comparison among four algorithms, the complexity of the proposed RBKSD is lower than that of SD when they both achieve the quasi-optimal performance. For instance, for K = 2, with slightly increase in complexity, the proposed RBKSD provides about 10dB gain over the KSD when SNR = 20dB. Furthermore, SD visited about 200 nodes while the proposed RBKSD searched about 90 nodes when reaching similar BER and Θ = 55%.

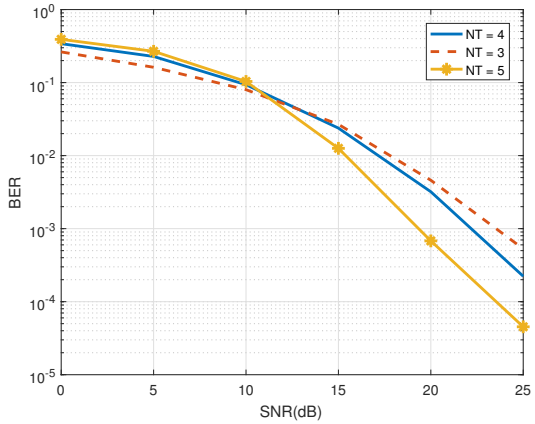

Fig. 4 BER performance of the proposed RBKSD with N_T = 3, 4, 5, R=2.

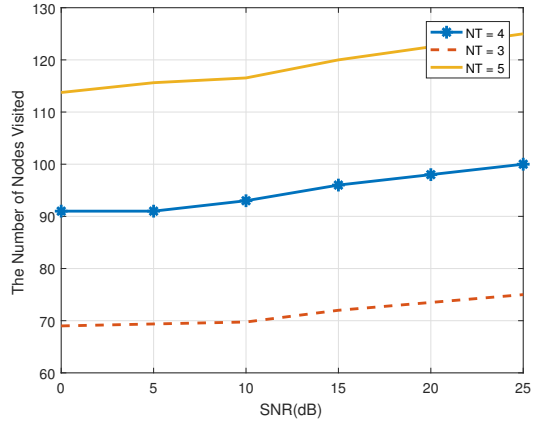

Fig. 5 Computational complexity of the proposed RBKSD with N_T = 3, 4, 5, R = 2.

In Fig. 4, we consider DUSTM with R = 2, N_T = 3, 4 and 5 for the proposed RBKSD. It can be found that the proposed RBKSD achieves a full diversity order for MIMO DUSTM system, which is consistent with the MLD. As is shown in Fig. 5, we compare the computational complexity of the proposed RBKSD with different number of transmit antennas. It can be found that the performance is improved with increasing number of transmit antennas, but the computational complexity is increased. Thus, for massive MIMO system, low-complexity detection methods must play an important role for its implementation.

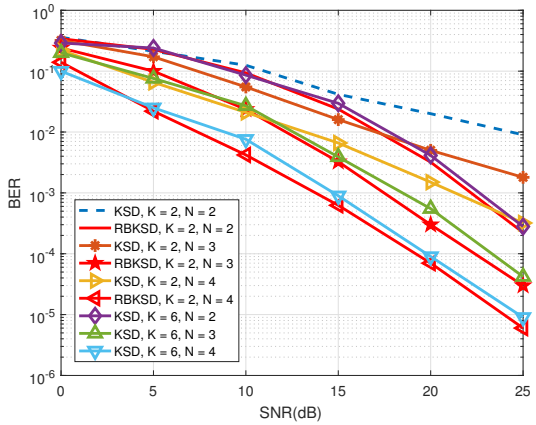

Fig. 6 BER performance comparison between the proposed RBKSD and KSD with N_T = 4, R = 2, K = 2, N = 2, 3, 4.

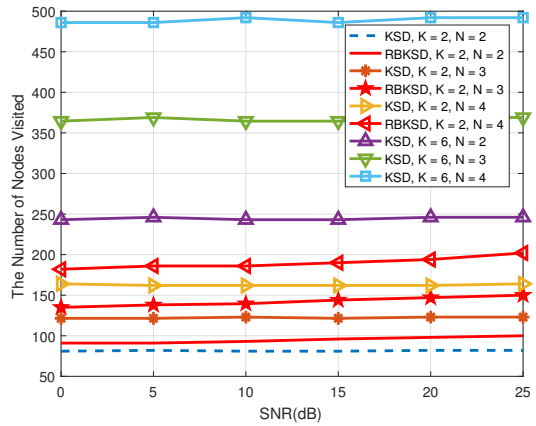

Fig. 7 Computational complexity comparison between the proposed RBKSD and KSD with N_T = 4, R = 2, K = 2, N = 2, 3, 4.

Fig. 6 and 7 gives the performance and complexity comparison of the proposed RBKSD and KSD for multi-symbol DUSTM systems. It is seen from Fig. 6 that the performance of the proposed RBKSD at the fixed threshold (K = 2, Γ = 0.28) performs much better than that of KSD with same K as N increases. And with the N (N = 3, 4, 5) increasing, an obvious increase in performance is observed obviously. Fig. 7 shows the computational complexity of both the proposed RBKSD and traditional KSD schemes. As seen, the complexity is increased with increasing N, but both the proposed RBKSD and KSD break the exponential computation complexity for MLD. Furthermore, the proposed RBKSD can greatly reduce the computational complexity in the case of the same performance. It can be seen that the proposed RBKSD shows the best trade-off between performance and complexity.

VI. Conclusion

In this paper, we proposed a Relaxed-Bound K-best sphere detection (RBKSD) for multi-antenna DUSTM system. Compared with the conventional KSD, the proposed RBKSD achieves the quasi-optimal performance at a reduced and roughly fixed complexity. Our main idea is to define a threshold Γ to overcome the disadvantages of the conventional KSD. It is proved by the simulation that the condition with the same index K, the proposed RBKSD algorithm significantly improves the system performance at the expense of slightly increasing the computational complexity. More importantly, if the near-optimal performance is guaranteed, the proposed RBKSD clearly obtains much lower complexity compared to the conventional KSD. Besides, compared with SD, the proposed RBKSD obtains almost the same performance via much lower complexity. Thus, utilization of the proposed RBKSD in DUSTM for massive MIMO would be also more attractive in comparison with other detection algorithms.

Acknowledgment

This work is supported by National Natural Science Foundation of China 61501461, and 61471269, National Major Project (No. 2015ZX03001013-002), Beijing Science and Technology Project (No. Z161100003016012), and the Early Career Development Award of SKLMCCS (Y3S9021F34).

References

[1] Yindi Jing and B.Hassibi, "Unitary space-time modulation via Cayley transform," *IEEE Trans. Signal Process.* vol. 51, pp. 2891−2904, Dec. 2003.

[2] Hui Ji, G. Zaharia and JF.Helard, "A New Differential Space-Time Modulation Scheme for MIMO Systems with Four Transmit Antennas," *ICT. 2013.* pp. 1−5, Oct. 2013.

[3] Chi−Hua Huang and Char-Dir Chung, "Differential Space-Time Modulation Using DAPSK Over Rician Fading Channels," *IEEE Wireless. Commun.* pp. 1−6, Jun. 2014.

[4] B. M. Hochwald and W. Sweldens "Differential Unitary Space-Time Modulation," *IEEE Trans. Commun*. vol. 48, pp. 2041−2052, Dec. 2000.

[5] Jibing Wang, M. P. Fitz and Kung Yao, "Differential unitary space-time modulation for a large number of receive antennas," *Conf. Record 36th Asilomar Conf. Signals, Syst. Computers, 2002*, vol. 1, pp. 565−569, Nov. 2002.

[6] S. N. Diggavi, N. Al-Dhahir, A. Stamoulis and A. R. Calderbank, "Differential space-time coding for frequency-selective channels," *IEEE Commun. Lett.* vol. 6, pp. 253−255, Aug. 2002.

[7] L. H. −J. Lampe, R. Schober, R. F. H. Fischer, "Coded differential space-time modulation for flat fading channels," *IEEE Trans. Wireless. Commun*. vol. 2, pp. 582−590, May. 2003.

[8] Cong Ling, Kwok Hung Li, A. C. Kot and Q. T. Zhang, "Multi-sampling decision-feedback linear prediction receivers for differential space-time modulation over Rayleigh fast-fading channels," *IEEE Trans. Commun*. vol. 51, pp. 1214−1223, Jul. 2003.

[9] Tao Cui and Chintha Tellambura, "Multiple-Symbol Differential Detection for Single-Antenna and Multiple-Antenna Systems over Ricean-fading Channels," *IEEE Int. Conf. Commun.* vol. 3, pp. 1439−1444, Dec. 2006.

[10] Ziyan Jia, Shiro Handa, Fumihito Sasamori and Shinjiro Oshita, "Multiple-Symbol Differential Detection for Unitary Space-Time-Frequency Coding," *IEEE Int. Conf. Circuits, Syst. Commun.* pp. 139−142, May. 2008.

[11] N. Jin, X. P. Jin, Y. G. Ying, S. Wang and Y. F. Lv, "Multiple-symbol M-bound intersection detector for differential unitary space‐time modulation," *IET. Commun.* vol. 4, pp. 1987−1997, Nov. 2010.

[12] V. Pauli and L. Lampe, "Tree-Search Multiple-Symbol Differential Decoding for Unitary Space-Time Modulation," *IEEE Trans. Commun.* vol. 55, pp. 1567−1576, Aug. 2008.

[13] Patrick K. M. Pun and Paul K. M. Ho, "Fano multiple-symbol differential detectors for differential unitary space-time modulation," *IEEE Trans. Commun.* vol. 55, pp. 540−550, Mar. 2007.

[14] Tao Cui and C. Tellambura, "Bound-intersection detection for multiple-symbol differential unitary space-time modulation," *IEEE Trans. Commun.* vol. 53, pp. 2114−2123, Dec. 2005.

[15] Cong Ling, Wai Ho Mow, K. H. Li and A. C. Kot, "Multiple-antenna differential lattice decoding," *IEEE J. Selected Areas.Commun.* vol. 23, pp. 1821−1829, Sept. 2005.

[16] Feifei Gao, Tao Cui, Arumugam Nallanathan and Chinthananda Tellambura, "Maximum Likelihood Detection for Differential Unitary Space-Time Modulation with Carrier Frequency Offset," *IEEE Trans. Commun.* vol. 56, pp. 1881−1891, Nov. 2008.

[17] Eunchul Yoon, "Maximum Likelihood Detection With a Closed-Form Solution for the Square QAM Constellation," *IEEE Commun. Lett.* vol. 21, pp. 829−832, Dec. 2017.

[18] Sinan Kahraman and M. Ertugrul Celebi, "Code based efficient maximum-likelihood decoding of short polar codes," *IEEE Int. Symposium, Information Theory Proceedings*, pp. 1967−1971, Aug. 2012.

[19] Ming-Xian Chang and Wang-Yueh Chang, "Efficient maximum-likelihood detection for the MIMO system based on differential metrics," *IEEE Wireless Commun.* pp. 603−608, Jun. 2015.

[20] Zhi Li, Xiang Cheng, Shuangshuang Han, Miaowen Wen, Liu-Qing Yang and Bingli Jiao, "A Low-Complexity Optimal SphereDecoder for Differential Spatial Modulation," *IEEE Global Commun. Conf.* pp. 1−6, Feb. 2016.

[21] Ti-wen Tang, Hsiao-ting Tien and Hsiao-feng Lu, "Coding schemes with constant sphere-decoding complexity and high DMT performance for MIMO multiple access channels with low-rate feedback," *IEEE Int. Symposium, Information Theory.* pp. 1902−1906, Aug. 2014.

[22] Yuehua Ding, Nanxi Li, Yide Wang, Suili Feng and Hongbin Chen, "Widely Linear Sphere Decoder in MIMO Systems by Exploiting the Conjugate Symmetry of Linearly Modulated Signals," *IEEE Trans. Signal Processing.* vol. 64, pp. 6428−6442, Aug. 2016.

[23] Ahmad A. Aziz El-Banna, Maha El-Sabrouty and Adel Abdelrahman, "Low Complexity Adaptive K-Best Sphere Decoder for 2x1 MISO DVB-T2," *ISWCS 2013.* pp. 1−5, Aug. 2013.

[24] Xin Wang, Ying Li and Jibo Wei, "An Improved Multiple-Symbol Differential Sphere Decoding for Differential Unitary Space-Time Modulation," *IEEE Singapore Int. Conf. Commun. Syst.* pp. 1−5, Nov. 2006.

[25] Chen Qian, Jingxian Wu, Yahong Rosa Zheng and Zhaocheng Wang, "A modified fixed sphere decoding algorithm for under-determined MIMO systems," *IEEE Global Commun. Conf.* pp. 4482−4487, Dec. 2012.

[26] Joakim Jalden and Petros Elia, "Sphere Decoding Complexity Exponent for Decoding Full-Rate Codes Over the Quasi-Static MIMO Channel," *IEEE Trans. Inf. Theory.* vol. 58, pp. 5785−5803, Jun. 2012.

[27] V. Pauli and L. Lampe, "Multiple-symbol differential sphere decoding for unitary space-time modulation," *IEEE Global Telecommun. Conf.* vol. 3, pp. 1630−1635, Dec. 2005.

[28] Chao Xu, Soon Xin Ng and Lajos Hanzo, "Multiple-Symbol Differential Sphere Detection and Decision-Feedback Differential Detection Conceived for Differential QAM," *IEEE Trans. Vehicular Technology.* vol. 65, pp. 8345−8360, Dec. 2015.